

INVESTIGATION OF WEAR AND CORROSION CHARACTERISTICS OF SHORT HEAT TREATED THIXOFORMED ALUMINIUM ALLOY

A.A. Rahman¹, M.S. Salleh¹, I.S. Othman¹, S. Subramonian¹,
S.H. Yahaya¹ and N. Siswanto²

¹Faculty of Manufacturing Engineering,
Universiti Teknikal Malaysia Melaka, Hang Tuah Jaya, 76100 Durian
Tunggal, Melaka, Malaysia.

²Department of Industrial Engineering,
Institut Teknologi Sepuluh Nopember, 60111
Surabaya, Indonesia.

Corresponding Author's Email: shukor@utem.edu.my

Article History: Received 21 August 2019; Revised 22 October 2019;
Accepted 22 December 2019

ABSTRACT: The thixoformed Al-Si-Cu alloys play an important role in automotive and engineering industries due to their wear resistance properties. This investigation looks into the wear and corrosion behaviors of thixoformed Al-Si-Cu alloy. Attempt has been made to relate the coefficient of friction (CoF) and corrosion rate on the short series of T6-heat treatment of thixoformed LM4 aluminium alloy. The short T6 heat treatment involves the application of solute solutioning, quenching and artificial ageing. Dry sliding condition using a pin-on-disc configuration against the SKD II steel disk under a constant load, distance and speed of 10 N, 1000 m and 0.1 m/s respectively was conducted to investigate the wear. The CoF of thixoformed shows an improvement of 5% where the T6 treated alloy is 0.4299 as compared to the 0.4537 untreated LM4 alloy. Furthermore, a significant reduction of 54% from 2.5459×10^{-4} mmpy to 1.1697×10^{-4} mmpy corrosion rate was also noted between the untreated and treated thixoformed alloy. Therefore, the alloys that undergone the short T6 heat treatment cycle generally improved the wear and corrosion resistant as compared to the alloys without heat treatment.

KEYWORDS: *Semisolid Metal Processing; T6-Heat Treatment; Coefficient of Friction; Wear; Corrosion Rate*

1.0 INTRODUCTION

Al-Si-Cu alloys such as LM4 possess excellent mechanical properties that make them suitable for many automotive components like cylinder blocks, piston, and camshaft cap. However, the conventional process that shows excessive primary silicon particle growth and

segregation, porosity and unfavourable shrinkage behaviour tends to limit their applications [1]. As-cast Al alloy is commonly known for its acicular-shaped eutectic silicon and coarse primary α -Al dendrite that reduces the mechanical properties and limits its applications. For instance, shrinkage is a classic problem in conventional casting due to its macrosegregation and porosity.

New development of aluminium alloys tailored for thixoforming provides an option that enhances the mechanical properties and reduces the problem associated with conventional casting [2]. One of the main requirements of thixoforming process requires the liquid to solid fractions of 0.3-0.5, which would ensure a laminar flow during forming process, hence reducing gas entrapment during solidification. Apart from thixoforming, grain refinement plays an important role in increasing the quality and reducing hot tearing of as-cast alloy. Several refinement methods, such as adding particles or alloying elements, enables grain size reduction and modification of its morphology from columnar to equiaxed grain [3-4].

Moreover, heat treatment has proven its ability to modify microstructures, with T6 heat treatment to be one of the most popular choices in increasing the hardness, strength, temperature resistance and ductility of a sample [5-7]. The T6 involves three stages which are solution treatment (ST), quenching and artificial aging [8-10]. ST is intentionally applied to dissolve the Cu-containing particles during solidification process and is carried out at a high temperature close to the eutectic temperature between 8-10 hours. However, many attempts were also conducted with a short ST time of between 2-4 hours [11-12]. This is proven possible by some research that produce the same material integrity while the ST time was reduced [8]. Even though the $Al_8Mg_3FeSi_6$ and $Al_5Cu_2Mg_8Si_6$ are hard to dissolve, it is sufficient to expose the LM4 alloy at high temperature in a short time to avoid local melting of Cu-containing phase during the solution treatment [13-15]. Although the enhancements of mechanical properties under T6 heat treatment have been discussed extensively, the influence of thixoforming and short T6 treatment on tribology of LM4 still remains unclear. Therefore, this study assesses the effect of the processes toward the tribology, coefficient of friction and corrosion rate of LM4 Al alloy.

2.0 METHODOLOGY

2.1 Thixoforming Processing

The billet was thixoformed using the T30-80KHz thixoforming apparatus. The primary material, LM4 aluminium alloy, in this project undergone similar work previously conducted that uses the cooling slope casting technique [16]. The thixoformed temperature of 580°C was selected from the liquid profiling that contained 50% liquid percentage based on the differential scanning calorimetry (DSC) test shown in Figure 1.

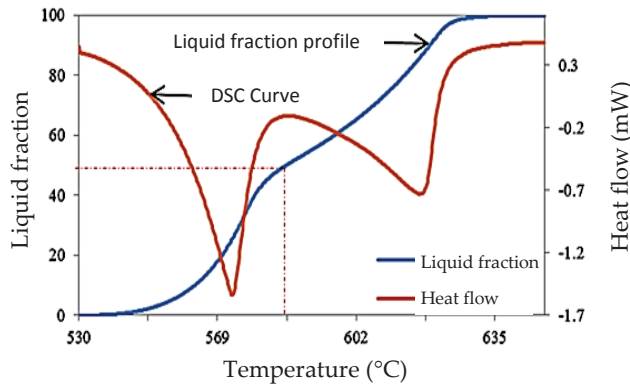


Figure 1: Differential scanning calorimetry (DSC) of heating flow and liquid profiling curves for LM4 aluminium alloy

A stainless steel mold was sprayed with silicon to increase flow ability during the forming process. The cooling slope LM4 feedstock shown in Figure 2 (a) was placed on the ram in the induction coil. The reheating process of the induction coil was controlled by using the current frequency, whereby an increment of 50 A per minutes was achieved until the intended thixoformed temperature, T_{thixo} was reached. As the billet temperature approaches T_{thixo} the ram was pushed upwards into the mould for the thixoforming process. A K-type thermocouple was used in this experiment to measure the billet temperature during processes. The thixoformed billet (Figure 2 (b)) from the mold was cooled at ambient temperature that would later undergo the short T6 heat treatment.

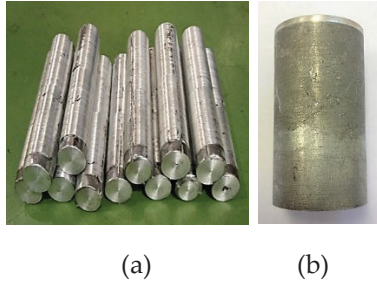


Figure 2: The LM4 aluminium alloy billet produced from (a) cooling slope process and (b) thixoforming process

2.2 Short T6 Treatment

Table 1 shows the T6 heat treatment temperature and time for heating the samples based on the ASM standards. The ST consists of solid-solutioning at 540°C for 60 minutes and followed by quenching in room temperature for 2 minutes, and aging treatment at 180°C for 120 minutes in the Nabertherm Furnace. The formation of globular microstructure of silicon particles take place after 5 minutes [9], therefore since the samples have undergone thixoforming process prior to T6, a shorter overall solution treatment was used instead. Furthermore, the formation of θ -phase reached the maximum hardness as no more formation of intermetallic phase was detected after 20 minutes.

Table 1: T6 heat treatment parameters

Solution Treatment	Quenching	Artificial Aging
540°C 60 minutes	27°C (room temp) 2 minutes	180°C 120 minutes

2.3 Wear Test

The wear test was conducted in accordance to ASTM-G99, the samples were machined by using an electrical discharge machine (EDM) wire cut to a 3 mm \varnothing x 30 mm length and later ground and polished at 350 rev/min. SKD II stainless steel (Figure 3) was used as the counter body while the alloy acted as a pin that was mounted to the pin and disc holder. The SKD II was cleaned by using an ultrasonic vibration in ethanol solution for 5 minutes.



Figure 3: SKD II stainless steel (counterbody)

Figure 4 shows the TR-20LE DUCOM Pin on Disc Tester, used to study the coefficient of friction (CoF) of LM4 Al alloy. The test was carried out with a sliding distance of 1000 m at 0.1 m/s sliding speed. All tests were performed at ambient temperature under normal load of 10 N. WINDUCOM software is used to plot and record all the frictional force data. The CoF was calculated from the frictional force data as shown in Equation (1) while the pin surface wear morphology characterization was then examined using SEM.

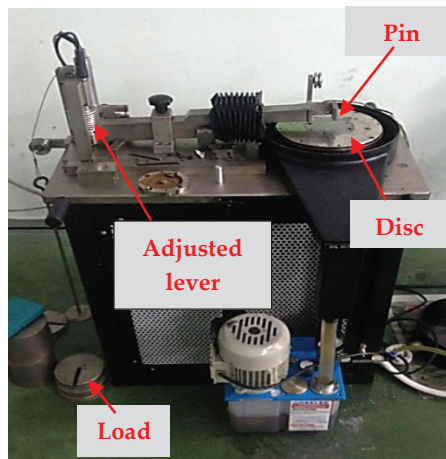


Figure 4: TR-20LE DUCOM pin on disc tester

$$\text{Coefficient of Friction, } \mu (\text{CoF}) = \frac{F}{W} \quad (1)$$

where F is a frictional force (N) and W is an applied load (N).

2.4 Corrosion Test

In order to study the corrosion rate of alloys, ASTM G69 standard practice was followed. AUTOLAB with glass cell of 10 mm² area was used to model the metal in the corroding system. The LM4 alloy was immersed in NaCl solution, as shown in Figure 5. Platinum electrode was used as the counter electrode while Ag-AgCl electrode was the

reference electrode. Distilled water was used to clean the electrode and glass cell after each testing. Samples were ground and polished before testing to ensure it is free from sites for pit initiation. A single Cu wire was welded on the other surface of the sample and connected to the working electrode to plot the current versus time graph during the test. Linear polarisation was selected in the procedure setup in Nova 10 software to control the corrosion parameter, as stated in Table 2.

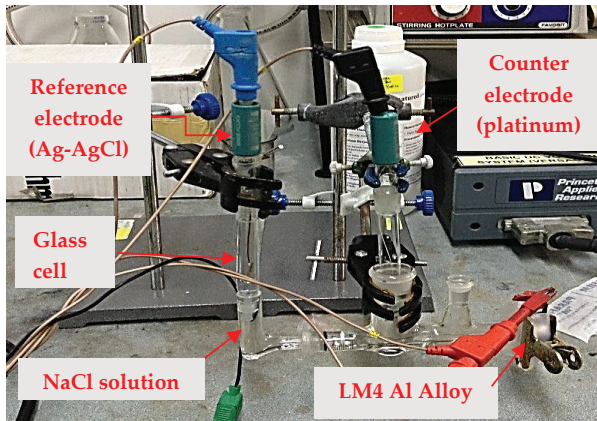


Figure 5: Glass cell setup for corrosion test

Table 2: Corrosion testing parameter

Corrosion test type: Glass cell	
Software	Nova 10
Corrosion area	1 mm ²
Solution	35 wt% of NaCl
Autolab control	10mA
OCP determination	120 s
LSV staircase	i. Start potential = -1 ii. Stop potential = 1 iii. Scan rate = 10 mV/s

Before testing was run, all wires were connected between the potentiostat and electrode was inserted into the glass cell. There were two colour indicators for the user to indicate whether to stop or continue the experiment. The green colour shows the corrosion reaction is still occurring while the red colour indicates that testing is over potential and the testing can be stop. Graphical output of log current density against the potential voltage was used to identify the I_{corr} ; thus, the corrosion rate (CR) was calculated from Equation (2).

$$\text{Corrosion rate, CR (mmpy)} = \frac{I_{corr} \times K \times EW}{p \times A} \quad (2)$$

where I_{corr} is the current corrosion, K is a corrosion constant and EW is an equivalent weight.

3.0 RESULTS AND DISCUSSION

3.1 Microstructural Evaluation

The Zeiss EVO 50 was used in the morphology analysis. Figure 6 (a) shows an untreated sample. It was clearly shown that the sample has near spheroidal microstructure with homogenous α -Al distribution surrounded by the Si eutectic. Figure 6 (b) shows the T6 treated sample which is seen to help increase the silicon particles spheroidisation and developed intragranular contrast during aging. The black dots in both morphologies determine that only small amount of eutectic are entrapped inside the globules. As a result of T6 heat treatment, the microstructure is coarser than the non-heat treated sample. Figure 7 shows the backscattered electrons of Si eutectic and α -Al with white and grey colour, respectively. It can also be seen that other intermetallic alloys are formed and have significant effect on the wear and corrosion rate. The $\text{Al}_{15}(\text{Fe},\text{Mn})_3\text{Si}_2$ had a Chinese script morphology. Meanwhile, the $\beta\text{-Al}_{15}\text{FeSi}$ has a needle-like shape and a small glowing trace due to the Fe compound. The $\beta\text{-Al}_{15}\text{FeSi}$ is not desirable due to the negative effect on the mechanical properties. Besides, small Al_2Cu particles can also be seen after the T6 heat treatment where it might be dissolved and spheroidised, and thus diffused into the surrounding matrix.

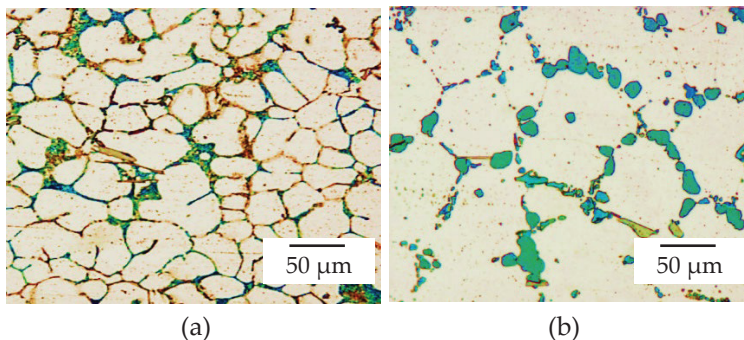


Figure 6: SEM morphologies of thixoformed alloy: (a) without heat treatment and (b) with T6 heat treatment

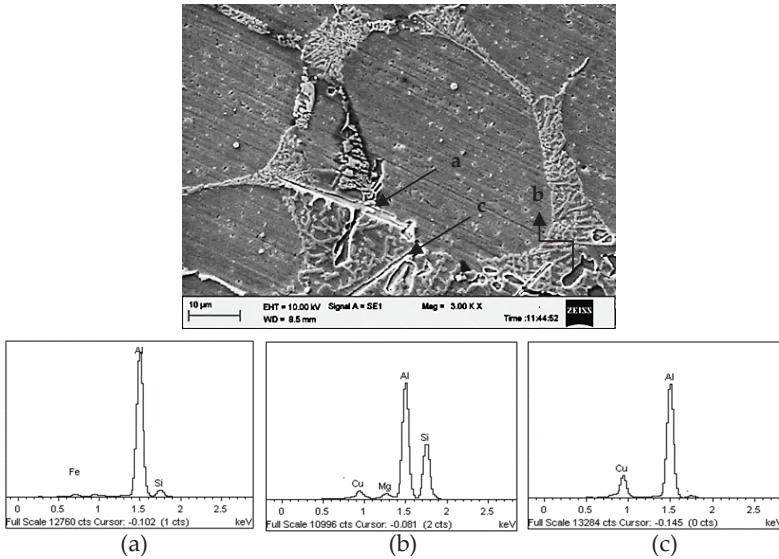


Figure 7: Backscattered electrons of T6 thixoformed Al alloy

3.2 Coefficient of Friction (CoF)

Figure 8 shows the wear tracks between T6 treated and untreated thixoformed LM4 Al alloy after sliding at 0.1 m/s which was caused by deformation and micro-ploughing of the soft LM4 Al alloy by hard SKD II steel counter body [17]. Since the wear test was conducted in dry conditions, increase in temperature may have led to metal softening, causing the severe plastic deformation and delamination experienced by the alloy [18]. Ribbon-like wear track confirmed that abrasion occurred during surface contact between LM4 pin and SKD II disc.

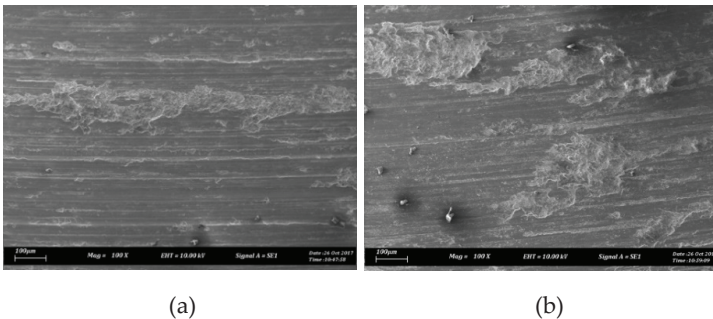


Figure 8: SEM of wear testing: (a) short T6 treatment and (b) untreated thixoformed LM4 Al alloy

Furthermore, shallow scratch particularly can be seen on worn surface of T6 LM4 Al alloy. The untreated LM4 also exhibit deep and non-

uniform grooves contrary to shallow and uniform grooves of T6 LM4 alloy. The deep grooves showed that excessive plastic deformation had happened. A possible explanation for these results may be the low hardness value of the untreated LM4 sample. Moreover, the stress imposed during the wear test has stimulated the Si particles fracture. The evidence of coarse silicon being pulled out from the matrix and leaving deep wear grooves with uneven distribution indicates that the primary Mg_2Si tends to remain in the matrix [18]. The enhancement in wear resistance was related to the finer Si particles; thus, reducing the CoF value for T6 as compared to untreated sample by 0.4299 and 0.4537 respectively. It indicates approximately a 5% improvement of the treated T6 sample as evidence of finer and smaller Si eutectic particles is observed in Figure 8 (a). Furthermore, non-heat treated LM4 sustained more severe damage with stratified structure aligned to the sliding direction as compared to the T6 heat treated alloy. It was believed that during dry sliding wear, the material was transferred from one surface to another which was caused by the contacting surfaces between the pin and counter body. The Si debonding particle dispersed in softer matrix thus affecting the wear resistance as shown in Figure 8 (b).

3.3 Corrosion Rate (CR)

Figure 9 shows the Butler-Volmer relation between potential and current density for the T6 and un LM4 alloys. Log current density was used to alter the wide range displayed during corrosion test. The anodic reaction will release the electrons which later speeds up the cathodic reaction causing counteracts on the initial perturbation of the corrosion system.

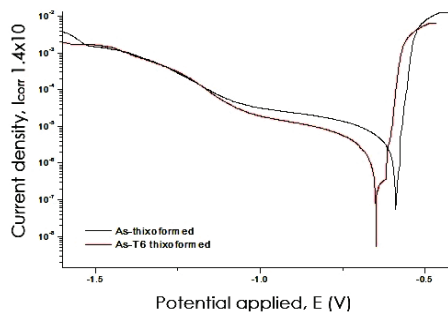


Figure 9: Current density vs potential applied for short T6 and untreated thixoformed LM4 Al alloy

CR for T6 treated reveals a 54% reduction from the untreated LM4 alloy value, where 1.1697×10^{-4} mmpy is achieved as compared to the untreated 2.5459×10^{-4} mmpy CR. Even though the oxide layer was

naturally formed on the LM4 alloy surfaces, Si eutectic formed during T6 heat treatment significantly helped to reduce the CR. Small CR value indicated that the pitting corrosion had hardly formed [19]. Furthermore, the Si eutectic and intermetallic spheroidisation during T6 heat treatment altered the macro-segregation that might form during a thixoforming process, and thus helped in increasing the corrosion resistance [20].

4.0 CONCLUSION

The study proves that the T6 heat treatment reduces wear by promoting more eutectic Si nucleation where a 5% lower CoF was recorded. During the wear test, eutectic Si particles produced hard and brittle surface in T6 treated LM4 alloy; thus, ensuring the α -Al was protected which consequently reduced wear significantly. The eutectic matrix microstructure of T6 heat treated alloys content also showed pronounced changes, particularly in size and morphology of the eutectic silicon which contributes to the wear and corrosion properties. The beneficial action of dissolution, spheroidisation and homogenization during solution treatment in T6 heat treatment also reduced the corrosion rate by 54% to 1.1697×10^{-4} mmpy; thus, improves the oxidation layer and material performance.

ACKNOWLEDGEMENT

The authors would like to thank Universiti Teknikal Malaysia Melaka (UTeM) and the Ministry of Education Malaysia for the financial support received under research grant FRGS/2018/FKP-AMC/F00379.

REFERENCES

- [1] A. Hekmat-Ardakana, X. Liu, F. Ajerscha and X.-Grant Chen, "Wear behaviour of hypereutectic Al-Si-Cu-Mg casting alloys with variable Mg contents", *Wear*, vol. 269, no. 9-10, pp. 684–692, 2010.
- [2] M.S. Salleh and M.Z. Omar, "Influence of Cu content on microstructure and mechanical properties of thixoformed Al-Si-Cu-Mg alloys", *Transactions of Nonferrous Metals Society of China*, vol. 25, no. 11, pp. 3523–3538, 2015.
- [3] M. Zhu, Z. Jian, G. Yang and Y. Zhou, "Effects of T6 heat treatment on the microstructure, tensile properties, and fracture behavior of the modified A356 alloys", *Materials and Design*, vol. 36, pp. 243–249, 2012.

- [4] K.T. Akhil, S. Arul and R. Sellamuthu, "The effect of heat treatment and aging process on microstructure and mechanical properties of A356 aluminium alloy sections in casting", *Procedia Engineering*, vol. 97, pp. 1676–1682, 2014.
- [5] K. Kashyap and T. Chandrashekar, "Effects and mechanisms of grain refinement in aluminium alloys", *Bulletin of Materials Science*, vol. 24, no. 4, pp. 345–353, 2001.
- [6] S.G. Shabestari and M. Malekan, "Assessment of the effect of grain refinement on the solidification characteristics of 319 aluminum alloy using thermal analysis", *Journal of Alloys and Compounds*, vol. 492, no. 1-2, pp. 134-142, 2010.
- [7] B.M. Afshari, S.S. Mirjavadi, Y.A. Dolatabad, M. Aghajani, M.K.B. Givi, M. Alipour and M. Emamy, "Effects of pre-deformation on microstructure and tensile properties of Al–Zn–Mg–Cu alloy produced by modified strain induced melt activation", *Transactions of Nonferrous Metals Society of China*, vol. 26, no. 9, pp. 2283–2295, 2016.
- [8] E. Sjölander and S. Seifeddine, "Optimisation of solution treatment of cast Al-Si-Cu alloys", *Materials and Design*, vol. 31, pp. S44–S49, 2010.
- [9] S. Menargues, E. Martín, M.T. Baile and J.A. Picas, "New short T6 heat treatments for aluminium silicon alloys obtained by semisolid forming", *Materials Science and Engineering A*, vol. 621, pp. 236–242, 2015.
- [10] M. Zeren, "Effect of copper and silicon content on mechanical properties in Al-Cu-Si-Mg alloys", *Journal of Materials Processing Technology*, vol. 169, no. 2, pp. 292–298, 2005.
- [11] D.A. Lados, D. Apelian and L. Wang, "Solution treatment effects on microstructure and mechanical properties of Al-(1 to 13 pct) Si-Mg Cast Alloys", *Metallurgical and Materials Transactions B*, vol. 42, no. 1, pp. 171–180, 2011.
- [12] J.H. Peng, X.L. Tang, J.T. He and D.Y. Xu, "Effect of heat treatment on microstructure and tensile properties of A356 alloys", *Transactions of Nonferrous Metals Society of China*, vol. 21, no. 9, pp. 1950–1956, 2011.
- [13] M.S. Salleh, M.Z. Omar, J. Syarif, K.S. Alhawari and M.N. Mohammed, "Microstructure and mechanical properties of thixoformed A319 aluminium alloy", *Materials and Design*, vol. 64, pp. 142-152, 2014.
- [14] Y. Birol, "Semi-solid processing of the primary aluminium die casting alloy A365", *Journal of Alloys and Compounds*, vol. 473, no. 1-2, pp. 133-138, 2009.
- [15] A.M.A. Mohamed and F.H. Samuel, "A review on the heat treatment of Al-Si-Cu/Mg casting alloys", in *Heat Treatment - Conventional and Novel Applications*, Rijeka, Croatia: InTech, 2012, pp. 55-72.

- [16] M.A.H. Safian, M.S. Salleh, S. Subramonian, N.I.S. Hussein, M.A. Sulaiman and S.H. Yahaya, "Production of feedstock for thixoforming using cooling slope casting", *Journal of Advanced Manufacturing Technology*, vol. 11, no. 1, pp. 77-90, 2017.
- [17] N. Saklakoğlu, S. Gencalp and S. Kasman, "The effects of cooling slope casting and isothermal treatment on wear behavior of A380 Alloy", *Advanced Materials Research*, vol. 264, pp. 42-47, 2011.
- [18] I. El Mahallawi, Y. Shash, R. M. Rashad, M. H. Abdelaziz, J. Mayer and A. Schwedt, "Hardness and wear behaviour of semi-solid cast A390 alloy reinforced with Al₂O₃ and TiO₂ nanoparticles", *Arabian Journal for Science and Engineering*, vol. 39, no. 6, pp. 5171–5184, 2014.
- [19] R. Arrabal, B. Mingo, A. Pardo, M. Mohedano, E. Matykina and I. Rodríguez, "Pitting corrosion of rheocast A356 aluminium alloy in 3.5 wt.% NaCl solution", *Corrosion Science*, vol. 73, pp. 342–355, 2013.
- [20] S. Tahamtan and A. Fadavi Boostani, "Evaluation of pitting corrosion of thixoformed A356 alloy using a simulation model", *Transactions of Nonferrous Metals Society of China*, vol. 20, no. 9, pp. 1702–1706, 2010.